



Marios Maroudas

Working Group: J. M. Batllori, Y. Gu, D. Horns, M. Maroudas, J. Ulrichs

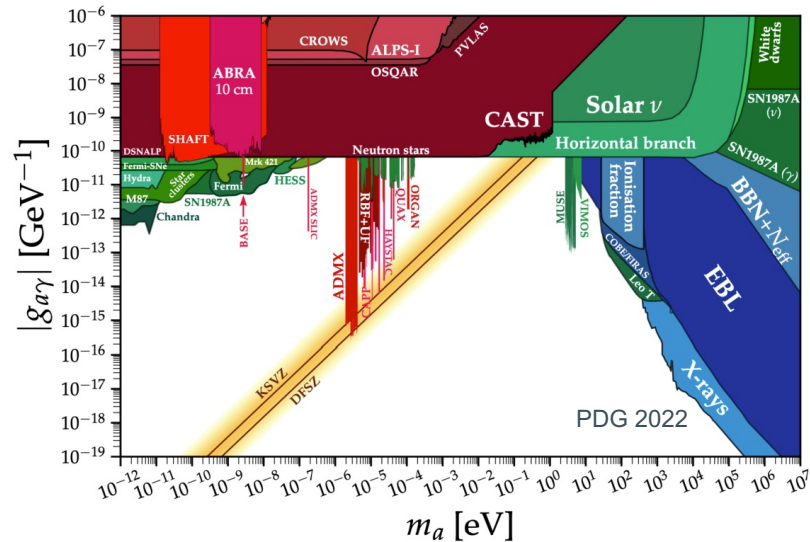
---

# WISP Searches on a Fiber Interferometer (WISPFI)



# Motivation

- Axions solve the strong CP problem and are prominent candidates for CDM [1].
- Haloscope experiments are very sensitive but depend on the local DM density → poorly constrained → could be substantially smaller [2].
- LSTW experiments are not sensitive to QCD axions (conversion scales with  $g_{a\gamma}^4$ ).
- High axion mass range (meV to eV) is unexplored by direct detection experiments (except CAST [3]).
- Null results of direct DM searches → Need for novel approaches!

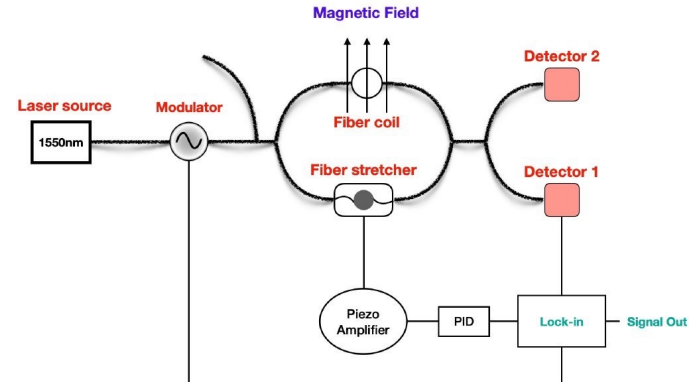


# WISPFI (WISP searches on a Fiber Interferometer)

- Novel table-top experiment focusing on **photon-axion conversion** in a waveguide by measuring **photon disappearance** in the presence of a strong external B field [4].
- Axion conversion probability scales with [5]:  
For  $P_{\gamma \rightarrow a} \ll 1$ :  $P_{\gamma \rightarrow a} \propto g_{a\gamma\gamma}^2 (BL)^2$
- Light guiding over **long distances & resonant detection** at a specially-confined region inside the bore of a strong magnet.
- **Mach-Zehnder interferometer** with the sensing arm inside the magnetic field.
- Expected signal: amplitude reduction & phase shift.

<https://doi.org/10.48550/arXiv.2305.12969>

- No local DM density dependence.
- Operation at room temperature (no cryogenic setup required).



# Photon-axion conversion

$$P_{\gamma \rightarrow a} = \underbrace{\sin^2(2\theta)}_{\text{Amplitude}} \underbrace{\sin^2(\pi L/L_{osc})}_{\text{Oscillations}} \quad [6]$$

Mixing angle:  $\tan(2\theta) = 2\omega \frac{g_{a\gamma\gamma} B}{k_\gamma^2 - k_a^2}$

Photon, axion wave momenta

- Maximum conversion occurs for **large energy  $\omega$**  or at  $\mathbf{k}_\gamma = \mathbf{k}_a$  (resonant conversion,  $\theta = 45^\circ$ ).
- Axion mass at resonance in a medium with effective refractive index  $n_{\text{eff}}$ :

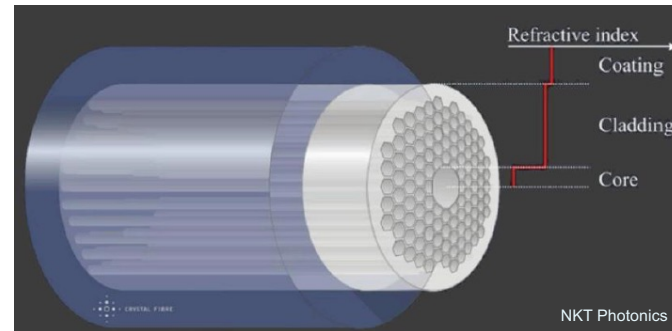
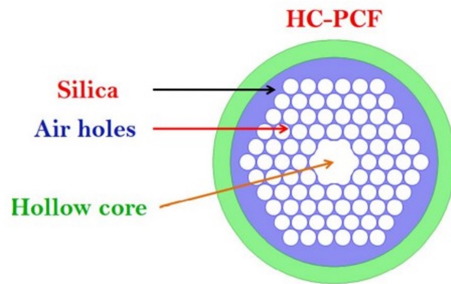
$$m_a = \omega \sqrt{1 - n_{\text{eff}}^2}$$

→ Required  $n_{\text{eff}} < 1$ !

- For  $P_{\gamma \rightarrow a} \ll 1$  the resulting probability becomes:  $P_{\gamma \rightarrow a} \approx 10^{-18} \left( \frac{g_{a\gamma\gamma}}{10^{-12} \text{ GeV}^{-1}} \right)^2 \left( \frac{B}{10 \text{ T}} \right)^2 \left( \frac{L}{200 \text{ m}} \right)^2$
- Energy ( $\omega$ ) independent!

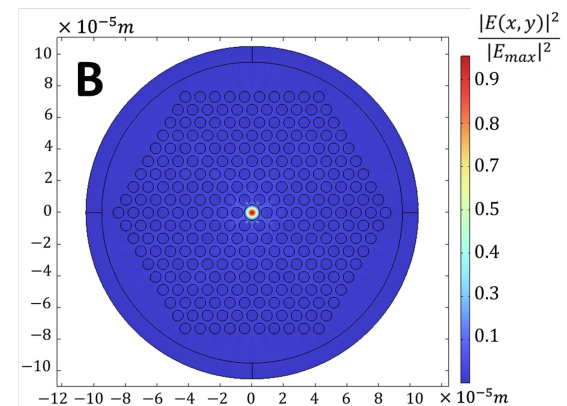
# Hollow-Core Photonic Crystal Fibers (HC-PCF)

- Resonant conditions can not be fulfilled for wave-guides based on dielectric materials.
- HC-PCF guide light through a low-refractive index hollow core which is surrounded by a periodic arrangement of air-holes in the cladding this generating a photonic-bandgap structure [7].
- Through the bandgap structure, the propagating mode can acquire  $n_{\text{eff}} < 1$  leading to real axion masses and resonant mixing.



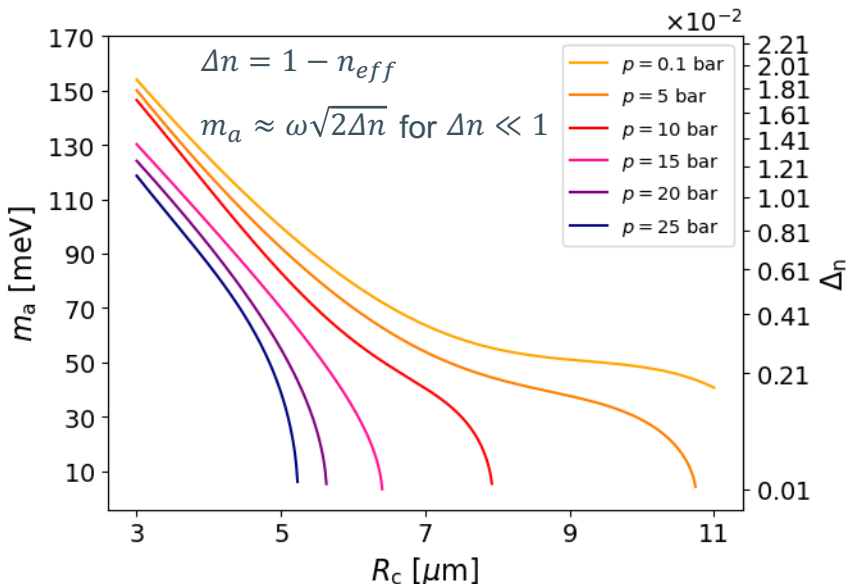
# Effective mode index in HC-PCF (I)

- $n_{\text{eff}}$  depends on the core radius ( $R_c$ ), the bending radius ( $R_b$ ), and the refractive index of the effective gas ( $n_{\text{gas}}$ ) which in turn depends on pressure ( $p$ ), wavelength ( $\lambda$ ), and temperature ( $T$ ) [8, 9].
- Analytical approximation [8]:  $n_{\text{eff}} = \frac{k_\gamma}{k_o} = \sqrt{n_{\text{gas}}^2(\lambda, p, T) - \left(\frac{u_{nm}}{k_\gamma R_c}\right)^2}$
- FEM simulations studying the actual fiber geometry.



Mode field distribution of HC-PCF  
 $(R_c = 5\mu\text{m}, p = 0.1\text{bar}, T = 20^\circ\text{C}, n_{\text{eff}} = 0.992, n_{\text{clad}} = 1.45)$

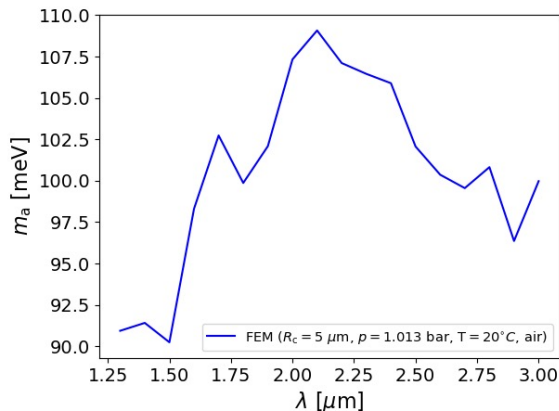
## Effective mode index in HC-PCF (II)



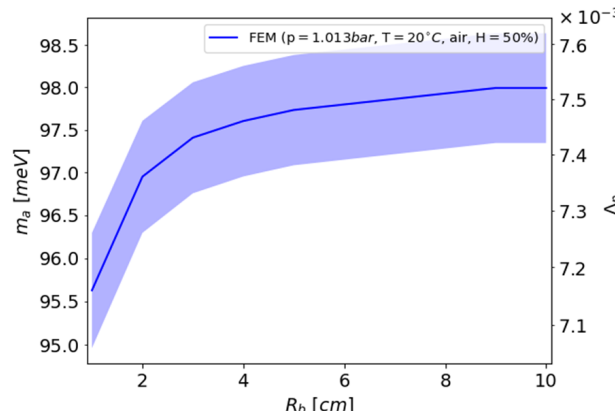
- Probed axion masses for resonant conversion based on different core radii ( $R_c$ ) and pressures ( $p$ ) of the air that fill the hollow core vary between  $\sim 10$  meV to 160 meV.
- Observed increase of  $n_{eff}$  with increasing  $R_c$  and  $p$  matches the analytical approximation.

# Effective mode index in HC-PCF (III)

- Wavelength of the propagating light and bending radius of the fiber also have an effect on the effective mode index.



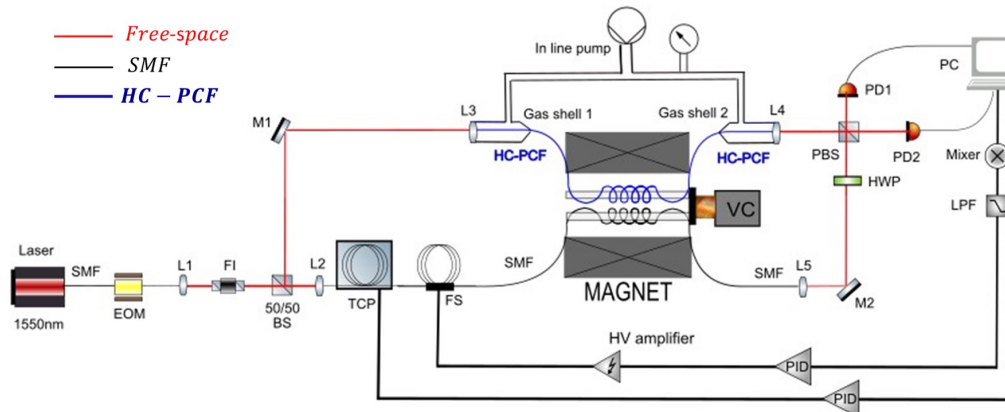
$$\Delta n = 1 - n_{eff} \quad m_a \approx \omega \sqrt{2\Delta n}$$



$$n'_{gas}(\lambda, p, T) = n_{gas}(\lambda, p, T) * n_{bend} = n_{gas}(\lambda, p, T) * \left( 1 + \frac{R_c}{R_b} \right)$$

# Experimental setup

- Partial free space partial fiber Mach-Zehnder-type interferometer.
- Sensing arm by HC-PCF placed in the magnetic bore and pressurized for tuning the probed axion mass.
- Both arms mounted on a voice coil (VC) for modulating the axion signal by shifting the position of the fiber coils and thus changing the effective B field.
- Fiber stretcher (FS) and temperature control pad (TCP) used for locking the interferometer via a PID.

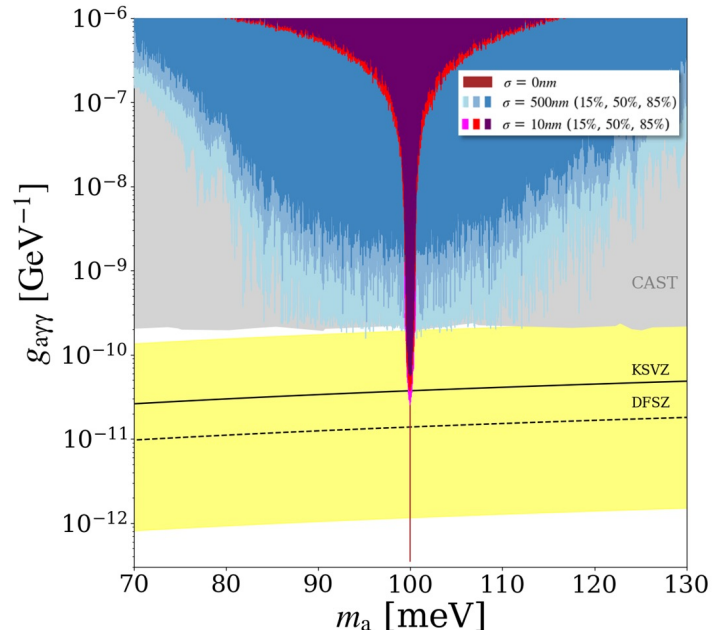


# Sensitivity (I)

- MZI operated at dark fringe.
- Instrumental noise dominated by the dark current of the photo-detector.
- No additional losses.

$$g_{a\gamma\gamma} \approx 4 \times 10^{-13} \text{ GeV}^{-1} \left( \frac{\text{SNR}}{3} \right)^{1/2} \left( \frac{B}{14T} \right)^{-1} \left( \frac{L}{500m} \right)^{-1} \left( \frac{P_{tot}}{4W} \right)^{-1/2} \left( \frac{\beta_{sig}}{1} \right)^{-1/2} \left( \frac{t}{180d} \right)^{-1/4} \left( \frac{\text{NEPPD}}{0.5fW/\sqrt{\text{Hz}}} \right)^{1/2}$$

- Axion mass mainly depends on core radius ( $R_c$ )
- HC-PCF production process leads to random variations of the  $R_c$  which widen the probed axion mass range but reduce the sensitivity.



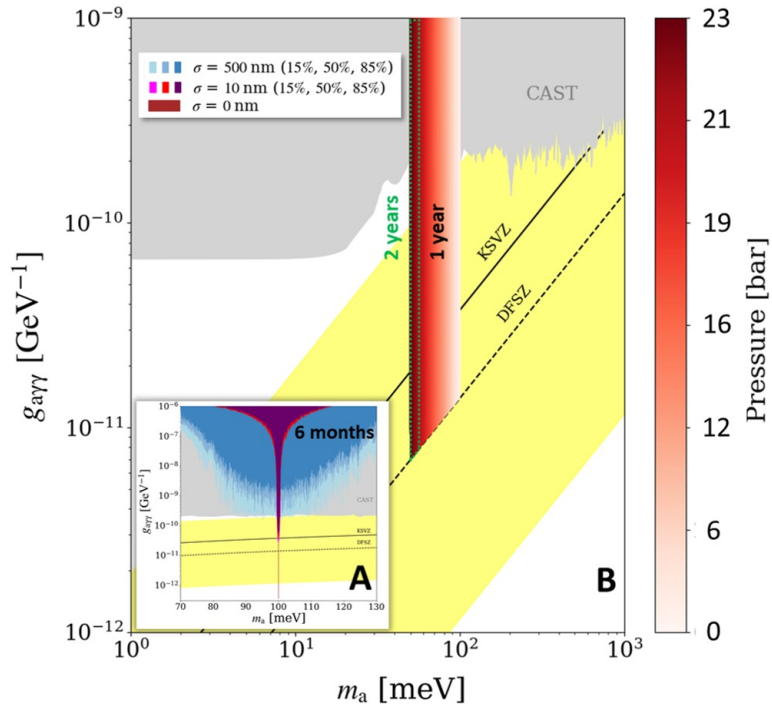
## Sensitivity (II)

A. Baseline setup: 4 W laser @ 1550 nm,  
 $B = 14$  T, 500 m HC-PCF at standard conditions.

B. Long term projection: 40 W laser @ 1550 nm,  
 $B = 14$  T, 1 km PM HC-PCF with  $\sigma=10$  nm.

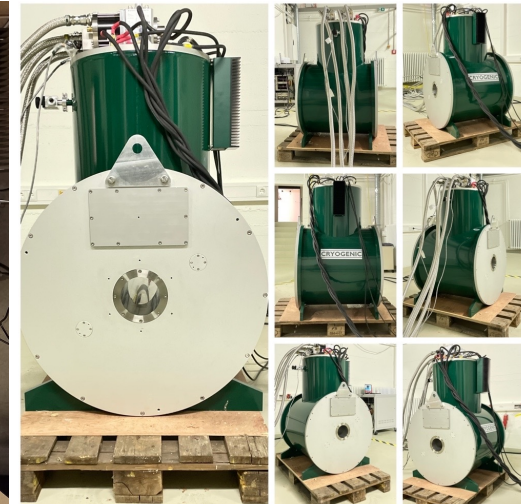
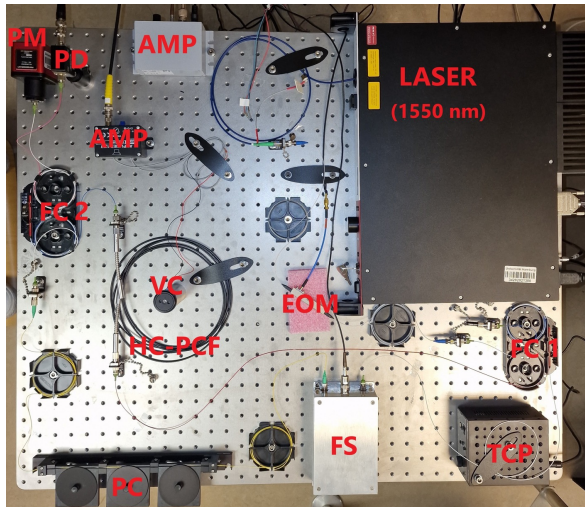
- Tuning from 0.1 – 23 bar in 116 steps of 0.6 meV between 50 – 100 meV

→ DFSZ sensitivity in a wide axion mass range!



# Future steps

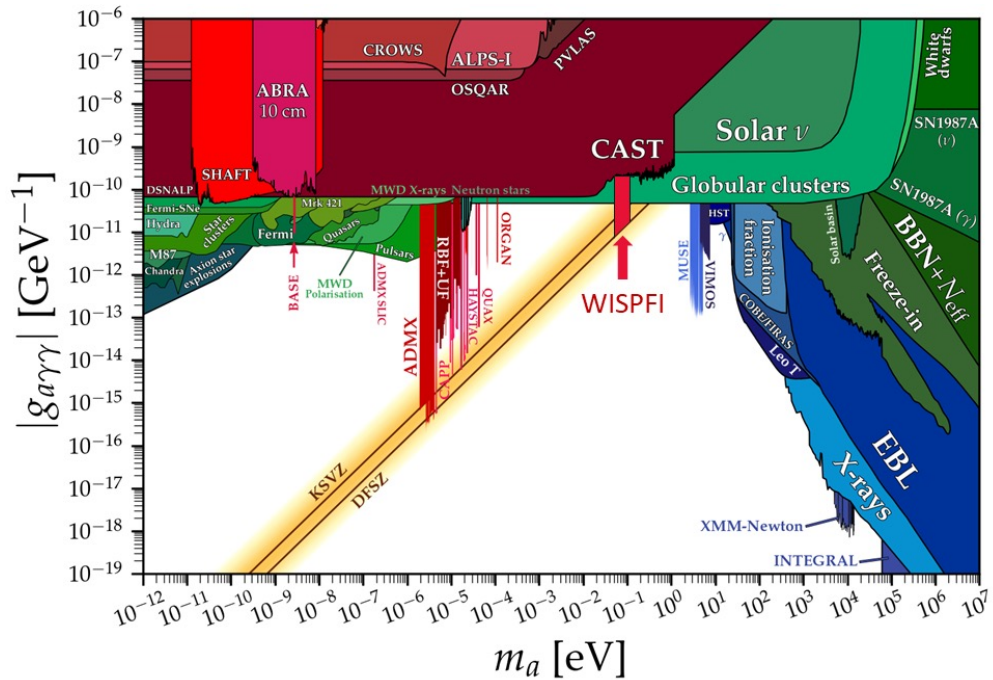
- Test HC-PCF fiber in the 14 T warm-bore solenoid magnet.
- Signal modulation with VC / wavelength modulation.
- Interferometer locking in amplitude/phase and temperature for larger fiber lengths (~100m).
- Integration to free-space.
- Noise optimization.
- Final commissioning and data acquisition.



# Summary

- Light guiding through **waveguide** embedded in a strong B field.
- Partial free-space, partial fiber **Mach-Zehnder**-type interferometer.
- **Amplitude/phase reduction/shift** in the presence of  $\gamma \rightarrow a$  conversion.
- **HC-PCF** meets the conditions for resonant mixing.
- **Tuning** in a wide axion mass range by regulating the **gas pressure** in the fiber.

<https://doi.org/10.48550/arXiv.2305.12969>





Universität Hamburg  
DER FORSCHUNG | DER LEHRE | DER BILDUNG

CLUSTER OF EXCELLENCE  
QUANTUM UNIVERSE



# Thanks for your attention!

Find out more about the cluster:  
[www.qu.uni-hamburg.de](http://www.qu.uni-hamburg.de)



# References

- (1) R. D. Peccei, H. R. Quinn, CP Conservation in the Presence of Pseudoparticles, Phys. Rev. Lett. 38, 1440 (**1977**),  
<https://doi.org/10.1103/PhysRevLett.38.1440>
- (2) B. Eggemeier et al., Axion minivoids and implications for direct detection, Phys. Rev. D 107, 083510 (**2023**),  
<https://doi.org/10.1103/PhysRevD.107.083510>
- (3) V. Anastassopoulos et al., New CAST limit on the axion-photon interaction, Nature Phys.13, 584-590 (**2017**),  
<https://doi.org/10.1038/nphys4109>
- (4) J. M. Batllori, et al, WISP Searches on a Fiber Interferometer under a Strong Magnetic Field, arXiv (**2023**),  
<https://doi.org/10.48550/arXiv.2305.12969>
- (5) H. Tam, Q. Yang, Production and detection of axion-like particles by interferometry, Phys. Lett. B, 716, 435-440 (**2012**),  
<https://doi.org/10.1016/j.physletb.2012.08.050>
- (6) G. Raffelt, L. Stodolsky, Mixing of the photon with low-mass particles, Phys. Rev. D 37, 1237 (**1988**),  
<https://doi.org/10.1103/PhysRevD.37.1237>
- (7) P. Russell, Photonic Crystal Fibers, Science 299, 5605 (**2003**), <https://doi.org/10.1126/science.1079280>
- (8) E. A. J. Marcatili, R. A. Schmeltzer, Hollow Metallic and Dielectric Waveguides for Long Distance Optical Transmission and Lasers, Bell System Technical Journal 43, 4, (**1964**), <https://doi.org/10.1002/j.1538-7305.1964.tb04108.x>
- (9) L. Rosa et al., Analytical Formulas for Dispersion and Effective Area in Hollow-Core Tube Lattice Fibers, Fibers 9, 10, (**2021**),  
<https://doi.org/10.3390/fib9100058>



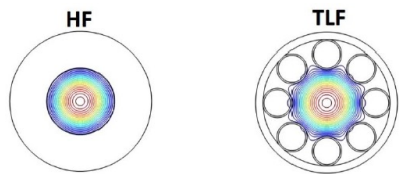
Universität Hamburg  
DER FORSCHUNG | DER LEHRE | DER BILDUNG

**CLUSTER OF EXCELLENCE**  
**QUANTUM UNIVERSE**

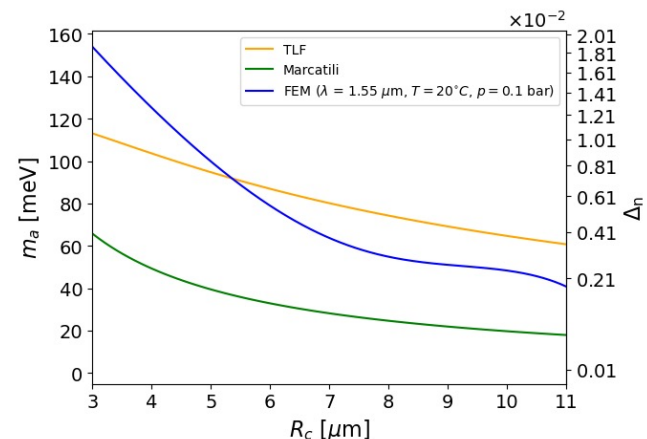
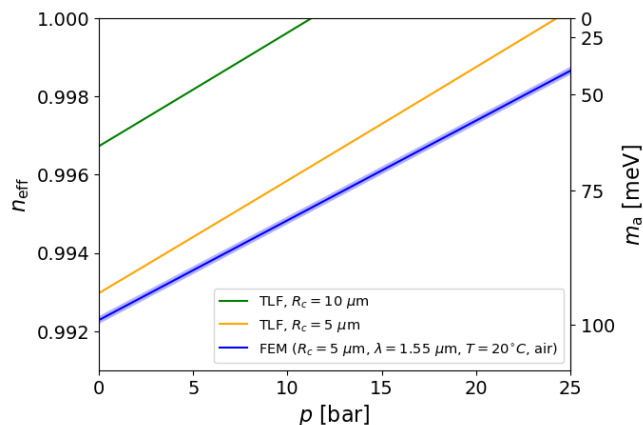


# Backup Slides

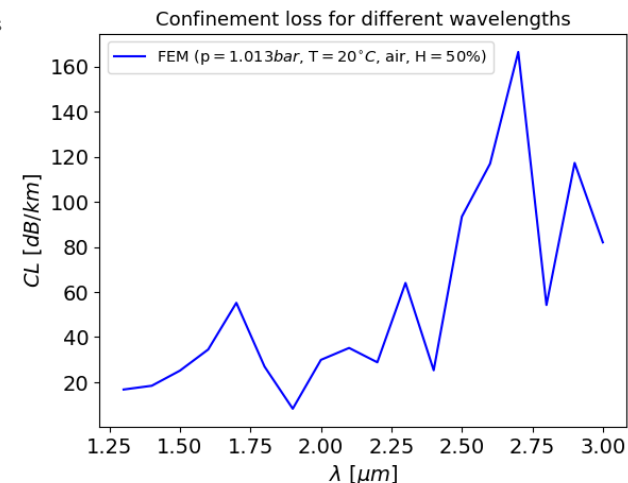
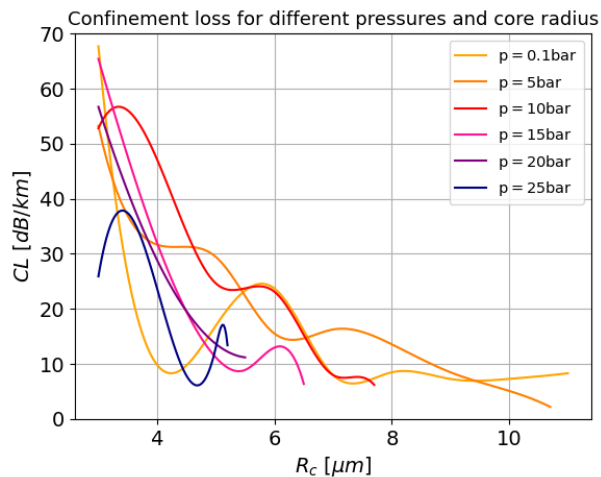
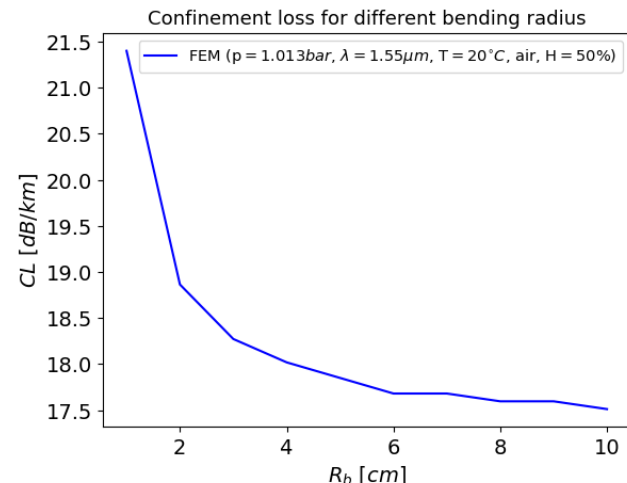
# Effective mode index in HC-PCF



$$n_{eff} = \frac{k_y}{k_o} = \sqrt{n_{gas}^2(\lambda, p, T) - \left( \frac{u_{nm}}{k_y R_c} \right)^2}$$



# Confinement losses



$$CL[dB/km] = -\frac{20}{\ln 10} \cdot \frac{2\pi}{\lambda} \cdot \text{Im}(n_{eff})$$

# Refractive index of air

- Refractive index of air as a function of pressure and temperature for  $T=20^{\circ}\text{C}$  and  $P=1.013 \text{ bar}$  accordingly.

